Inhalation Toxicology, 18:313–332, 2006

ISSN: 0895-8378 print / 1091-7691 online
DOI: 10.1080/08958370500515871

Taylor & Francis
Taylor & Francis Group

The Toxicological Response of Brazilian Chrysotile Asbestos: A Multidose Subchronic 90-Day Inhalation Toxicology Study with 92-Day Recovery to Assess Cellular and Pathological Response

David M. Bernstein
Consultant in Toxicology, Geneva, Switzerland

Rick Rogers
Rogers Imaging Corporation, Needham, Massachusetts, USA

Paul Smith
Research & Consulting Company Ltd., Füllinsdorf, Switzerland

Jörg Chevalier
EPS Experimental Pathology Services AG, Muttenz, Switzerland

Inhalation toxicology studies with chrysotile asbestos have in the past been performed at exceedingly high doses without consideration of fiber number or dimensions. As such, the exposures have exceeded lung overload levels, making quantitative assessment of these studies difficult if not impossible. To assess the cellular and pathological response in the rat lung to a well-characterized aerosol of chrysotile asbestos, a 90-day subchronic inhalation toxicology study was performed using a commercial Brazilian chrysotile (CA 300). The protocol was based on that established by the European Commission for the evaluation of synthetic vitreous fibers. The study was also designed to assess the potential for reversibility of any such changes and to permit association of responses with fiber dose in the lung and the influence of fiber length. Wistar male rats were randomly assigned to an air control group and to 2 CA 300 exposure groups at mean fiber aerosol concentrations of 76 fibers $L > 20$ μm/cm^3 (3413 total fibers/cm^3; 536 WHO fibers/cm^3) or 207 fibers $L > 20$ μm/cm^3 (8941 total fibers/cm^3; 1429 WHO fibers/cm^3). The animals were exposed using a flow-past, nose-only exposure system for 5 days/wk, 6 h/day, during 13 consecutive weeks (65 exposures), followed by a subsequent nonexposure period lasting for 92 days. Animals were sacrificed after cessation of exposure and after 50 and 92 days of nonexposure recovery. At each sacrifice, subgroups of rats were assessed for the determination of the lung burden; histopathological examination; cell proliferation response; bronchoalveolar lavage with the determination of inflammatory cells; clinical biochemistry; and for analysis by confocal microscopy. Through 90 days of exposure and 92 days of recovery, chrysotile at a mean exposure of 76 fibers $L > 20$ μm/cm^3 (3413 total fibers/cm^3) resulted in no fibrosis (Wagner score 1.8 to 2.6) at any time point. The long chrysotile fibers were observed to break apart into small particles and smaller fibers. In vitro modeling has indicated that these particles are essentially amorphous silica. At an exposure concentration of 207 fibers $L > 20$ μm/cm^3 (8941 total fibers/cm^3) slight fibrosis was observed. In comparison with other studies, chrysotile produced less inflammatory response than the biosoluble synthetic vitreous fiber CMS. As predicted by the recent biopersistence studies on chrysotile, this study clearly shows that at that at an exposure concentration 5000 times greater than the U.S. threshold limit value of 0.1 f(WHO)/cm^3, chrysotile produces no significant pathological response.

Received 16 September 2005; accepted 16 November 2005.
This study was sponsored by a grant from SAMA Mineraçào de Amianto LTDA. Brazil.
Address correspondence to Dr. David M. Bernstein, Consultant in Toxicology, 40 chemin de la Petite-Boissière, 1208 Geneva, Switzerland. E-mail: davidb@itox.ch

Recent inhalation biopersistence studies have shown that chrysotile clears very rapidly from the lung. These studies have provided a distinctive mechanistic basis for the differentiation of chrysotile, a serpentine mineral, from amphibole asbestos. However, they remained in contradiction to the chronic inhalation toxicology studies of chrysotile, which were performed at very high exposure concentrations (10 mg/m^3) and which resulted in a tumorigenic response. Recently, these studies were evaluated in detail and found to meet the paradigm for lung overload, thus making quantitative assessment of these studies difficult if not impossible (Bernstein, 2005). It should be noted that some studies not using the EC inhalation biopersistence protocol have shown that chrysotile clears more slowly (e.g., Coin et al., 1992). As presented later in the discussion, these studies have also been performed at extremely high chrysotile concentrations, "10 mg (respirable)/m^3," and used a special chrysotile sample that was heavily pulverized, making extrapolation of the results nearly impossible.

A recent working group evaluating short-term assays and testing strategies for all types of fibers stated, "Thus the database on the links between in vitro biopersistence, in vivo biopersistence, and pathologic effects is derived for the limited class of silica-based fibers. The extent to which this understanding of biopersistence that we have gained for these fibers is generalizable to other fibers (e.g. organic fibers, crystalline fibers, non oxide fibers is not known and more research is needed before we use the same paradigm for these other fibers types" (ILSI, 2005, p. 508). For these other fibers, the ILSI working group recommended a tiered approach, which included as one of the optional endpoints biopersistence, and recommended subchronic inhalation toxicology study to investigate biological activity.

To evaluate the toxicological response to chrysotile, a multidose, subchronic, 90-day inhalation toxicology study was performed on Brazilian chrysotile using a well-characterized aerosol. The chrysotile used in this study is the same as evaluated in the inhalation biopersistence study (Bernstein et al., 2004). The protocol used for this study followed that established by the European Commission for the evaluation of synthetic mineral fibers (Bernstein & Riego-Sintes, 1999; Bellmann et al., 2003) with the exception of the fiber counting and sizing rules. These were adapted to the use of transmission electron microscopy (TEM) in order to assure detection of the chrysotile fibers. In addition, the lungs were analyzed using confocal microscopy in order to provide a noninvasive assessment of fiber distribution and cellular response.

MATERIALS AND METHODS

The exposure and in-life phases of the study were performed at the Research and Consulting Company Ltd., Füllinsdorf, Switzerland. Fiber counting and sizing were performed under subcontract to RCC at Gesellschaft für Staubmesstechnik und Arbeitsschutz GmbH (GSA), Neuss, Germany. The confocal microscopy analysis was performed by Rogers Imaging Corporation, Needham, MA.

Fiber Samples

The chrysotile fibers used in this study were obtained from the Cana Brava Mine, located in Minasu in the state of Goias in Brazil.

The chrysotile fiber is monoclinic in crystalline structure and has a unique rolled structure, described later. The fibers are present in the mine in all length categories, ranging from "long" (greater than 10 mm: grades 4T, 4K, 4A, and 3T on the Canadian Quebec Screening Scale [QSS]; Cossette & Delvaux, 1979), to medium (fibers between 5 and 9 mm: QSS grades 4X, 4Z, and 5K), to "short" (below 5 mm: QSS grades 5R, 6D, 7M, and 7T).

The chemical composition and the structure of chrysotile are markedly different from that of amphiboles such as tremolite or amosite (Hodgson, 1979), as shown in Table 1.

Characterization of Fiber Sample

The stock chrysotile fibers used in this study were from the same batch as used in the inhalation biopersistence study (Bernstein et al., 2004). The mean dimensions of the stock fibers are shown in Table 2.

The fiber exposure concentrations were initially chosen based on a prestudy calibration trial to be 50 and 150 fibers/cm^3, which correspond in the EC subchronic fiber inhalation protocol (Bernstein & Riego-Sintes, 1999) to the medium and high dose levels recommended for exposure. However, due to variation in the distribution of the stock fiber, the mean high dose

TABLE 1
Typical chemical composition of chrysotile and the amphiboles tremolite and amosite (percent)

Compound	Chrysotile[a]	Tremolite[b]	Amosite[b]
SiO_2	40.90	55.10	49.70
Al_2O_3	5.88	1.14	0.40
Fe_2O_3	6.85	0.32	0.03
FeO	—	2.00	39.70
MnO	—	0.10	0.22
MgO	34.00	25.65	6.44
CaO	Trace	11.45	1.04
K_2O	0.02	0.29	0.63
Na_2O	0.03	0.14	0.09
H_2O^+	[c]	3.52	1.83
H_2	[c]	0.16	0.09
CO_2	[c]	0.06	0.09
Ignition loss[c]	12.20		
Total	99.95	99.93	100.26

[a]Cana Brava Mine.

[b]Hodgson (1979, pp. 80–81).

[c]H_2O^+, H_2, and CO_2 were included together as ignition loss in the analysis.

TABLE 2
Dimensions of the chrysotile stock fibers

WHO fibers of total fibers (%)	Fibers $L > 20\ \mu$m of total fibers (%)	Fibres L 5–20 μm of total fibers (%)	fibers $L < 5\ \mu$m of total fibers (%)	Diameter range (μm)	Length range (μm)	Diameter mean ± SD (μm)	Length mean ± SD (μm)	GMD (μm)	GSD-D	GML (μm)	GSD-L	Aspect ratio
15.1%	1.4%	13.9%	84.7%	0.03 – 0.7	0.8 – 90	0.17 ± 0.1	3.53 ± 14.09	0.15	1.86	2.55	4.15	28.4

fiber (f) exposure concentration was 207 f/cm^3 $L > 20\ \mu$m and the medium dose was 76 f/cm^3 $L > 20\ \mu$m.

The nomenclature of "medium" and "high" dose levels is used throughout this publication so as to correspond to the groups as recommended in the EC protocols and to facilitate comparison in the discussion with other exposures performed using the EC protocol.

EXPERIMENTAL DESIGN

The experimental design of this study was based on the protocol established by the European Commission for evaluating the subchronic response to synthetic mineral fibers (Bernstein & Riego-Sintes, 1999).

Animal Exposure

Groups of 39 (9-wk-old) male Wistar Han-Ibm outbred rats (SPF quality) were exposed by flow-past nose-only exposure to mean fiber aerosol concentrations of 76 and 207 fibers $L > 20\ \mu$m/cm^3 for 6 h/day, 5 days/wk, for a period of 13 consecutive weeks. In addition, a negative control group was exposed in a similar fashion to filtered air.

Exposure System

The fiber aerosol generation system was designed to loft the bulk fibers without breaking, grinding or contaminating the fibers (Bernstein et al., 1994). The animals were exposed by the flow-past nose/snout-only inhalation exposure system. This system was derived from Cannon et al. (1983) and is different from conventional nose-only exposure systems in that fresh fiber aerosol is supplied to each animal individually and exhaled air is immediately exhausted.

Clinical Observations

All animals were observed for mortality/morbidity before the start and after the completion of each exposure and at least once on nonexposure days, including the quarantine phase, the acclimatization phase, and the postexposure observation phase. A detailed clinical observation for toxicological signs, including the time of onset, intensity, and duration, was performed on all animals on the first day of the acclimatization phase, on the first day of the exposure (before exposure), twice weekly during the exposure phase (before the daily exposure), on the first day of the postexposure period, and weekly thereafter.

Body Weights

Body weights were recorded once at the beginning of the acclimatization period, on the day of first exposure, prior to exposure start, and then weekly throughout the exposure phase on the first day of the postexposure period, and every second week thereafter.

Disease Surveillance

Nonheparinized blood samples (approximately 1 ml) were obtained by retro-orbital puncture under light ether anesthesia from six additional animals. The blood was immediately forwarded to the Department of Microbiology (at RCC). Serum was obtained by centrifugation of blood. Aliquots from serum were used for screening for the presence of antibodies to the following rodent pathogens: Hantaan virus, *Bacillus piliformus* (Tyzzer's), lymphocytic choriomeningitis virus (LCM), Kilham rat virus (KRV), pneumonia virus of mice (PVM), reovirus type 3 (Reo3), sialodacryoadenitis (SDA)/rat coronavirus (RCV), Sendai virus (parainfluenza-1 virus), Toolan (H-1), *Mycoplasma pulmonis*, and minute virus of mice (MVM). None of these pathogens was found.

Lung Burden, Histopathology and Cell Proliferation

Proliferating cells were labelled by 5-bromo-2′-deoxyuridine (BrdU) using a mini-osmotic pump, which was implanted 3 days before sacrifice. Five rats from each time point and sacrifice were anesthetized by inhalation of Halothane delivered to a face mask from a vaporizer. A BrdU-filled osmotic mini-pump (ALZET 2001) was then surgically implanted into a subcutaneous pocket, in order to quantify cell turnover (Alza Corp. model 2001; flow rate 1 μl/h, BrdU concentration = 50 mg/L). The BrdU proliferation in the terminal bronchial region, in the lung parenchyma, and in the pleura was determined on 3 rats each from the control and the high-dose exposure group at 92 days after cessation of exposure.

Lungs. The lungs and trachea (sectioned below the larynx) were removed with the attached mediastinal tissue. The mediastinal tissue containing the mediastinal lymph nodes was resectioned from the lung lobes and fixed in formalin and archived at the disposal of the sponsor. The remaining

tissue/organs—lower half of the trachea, main stem bronchi, and lung lobes—were weighed (recorded as "lung, whole").

Right Lung Lobes. For analysis of fiber content following digestion by low-temperature ashing, the bronchus leading to the right lung lobe was removed, leaving as little bronchial tissue as possible on the lobes. The lobes were weighed (recorded as "right lung lobes") separately and inserted into a plastic bag and deep-frozen (–20°C).

Left Lung Lobe. For histopathology, the main-stem bronchus of the left lung lobes was removed just above the point of bifurcation. The left lung was weighed (recorded as "left lung lobe"), then fixed in 10% neutral buffered formalin solution by instillation under a pressure of 30 cm H_2O and immersion for 2 h, and subsequently stored in formalin. A short piece of duodenum was taken and fixed with the left lung lobes in formalin. The left lobe remained in the formalin fixation for no more than 48 h. At this time the lobe was frontally trimmed. The dorsal half was transferred to 70% ethanol, along with the piece of duodenum, dehydrated, embedded in paraffin wax, and stored for immunohistochemical staining for evaluation of the proliferative response. The frontal half was replaced in formalin until processed, embedded, and cut at a nominal thickness of 4 μm. Two sets of slides were prepared: One set was stained with hematoxylin and eosin for histopathological examination, and the second set was stained with trichrome for collagen specific analysis. The trachea was processed, embedded, cut at a nominal thickness of 4 μm and stained with hematoxylin and eosin.

Slides of the frontal left lung lobe and of the trachea were examined histopathologically by Dr. H. J. Chevalier, EPS. Chronic pulmonary changes and fibrosis were evaluated according to the grading system presented by McConnell and Davis (2002). In addition, the amount of collagen deposition at the bronchoalveolar junctions was presented as a grade from 0 to 5 as described in the annex of the EU guidelines (Bernstein & Riego-Sintes, 1999).

Bronchoalveolar Lavage

On separate subgroups of animals, bronchoalveolar lavage was performed. The lungs were washed 6 times with 4 ml physiological saline at room temperature by slow instillation and withdrawal of fluid, with thoracic massage. The total amount of lavage fluid collected was recorded. The lavage fluid from the first two lavages was collected in a centrifugation tube on ice. The recovered volume from this wash was recorded. This fluid was centrifuged at approximately 300 × g for 10 min at ~4°C. The supernatant was transferred to a plastic tube and analysed for enzymatic activity of lactate dehydrogenase (LDH), beta-glucuronidase (ß-GRS), and for determination of total protein. The following methods and instrumentation were used to determine the parameters listed:

Parameter	Method/instrumentation	Unit
Lactate dehydrogenase (LDH)	UV-kinetic, measurement of the rate of decrease in NADH (direct NADH/LDH coupled reaction using pyruvate as substrate (PYR → LACT reaction). Method based on German Society of Clinical Chemistry (DGKC) recommendations (BM/Hitachi 917 discrete random access analyzer).	μkat/L (37°C)
β-Glucuronidase (β-GRS)	Colorimetric assay based on the hydrolysis of the substrate phenolphthalein mono-β-glucuronic acid by β-GRS with the release of free phenolphthalein. The intensity of the color produced is directly proportional to the enzyme activity in the sample (Pharmacia Biotech Ultrospec 3000 UV/VIS Spectrophotometer).	U/ml (56°C)
Protein, total	Turbidimetric assay, using benzethonium chloride to react with protein in a basic medium (BM/Hitachi 917 discrete random access analyzer).	mg/L

The lavage fluid from the 4 further lavages was pooled in a centrifugation tube, the volume recorded and centrifuged at approximately 300 × g for 10 min at ~4°C. The supernatant was discarded. The cell pellets were each resuspended with physiological saline and pooled. The volume was recorded in the raw data. The total volume was gently shaken for mixing. Aliquots of the cell suspension were taken for total cell count, cell viability, and differential cell counting, as described next.

Total Cell Count. An aliquot of the cell suspension was diluted in Türk's stain (Diagnostik Merck no. 9277, Merck AG, Darmstadt/Germany). An aliquot of this mixture was introduced into a hemocytometer chamber, and the total cell was counted (at least 1 mm^3).

Cell Viability Assay. An aliquot of 50 μl of the cell suspension was mixed with 12.5 μl of a 0.4% aqueous Trypan blue solution and pipetted into a hemocytometer chamber. Within 5 min of mixing, at least 200 cells were assessed for viability.

Differential Cell Count. According to the results of the total cell count, an aliquot of cell suspension was diluted with physiological saline solution to give an end concentration of approximately 1 million cells/ml. From this suspension a smear was prepared using a cytocentrifuge (Shandon, Instrument Gesellschaft AG, Switzerland) and stained with Diff-Quick (Baxter Dade, Switzerland). At least 500 cells per smear were counted by light

microscopy. The numbers of each cell type—macrophages, neutrophils, lymphocytes, eosinophils, epithelial cells, and other cells—were assessd.

Lung Digestion for Fiber/Particle Analysis

From five rats per group per time point in the CA300 exposure group and air control exposure group the lungs were thawed and the entire lung was prepared for analysis. The tissue was initially dehydrated by freeze drying (Edwards EF4 Modulyo freeze dryer) and dried to constant weight to determine the dry weight of the tissue. The dry tissue was plasma ashed in an LFE LTA 504 multiple chamber plasma unit at 300 W for at least 16 h. Upon removal from the ashing unit, the ash from each lung was weighed and suspended in 10 ml methanol using a low-intensity ultrasonic bath. The suspension was then transferred into a glass bottle with the combustion boat rinse and the volume was made up to 20 ml. An aliquot was then removed and filtered onto a gold-coated polycarbonate filter (pore size 0.2 μm).

Counting Rules for the Evaluation of Air and Lung Samples by Transmission Electron Microscopy

All fibers visible at a magnification of 10, 000$\times$ were taken into consideration. All objects seen at this magnification were sized with no lower or upper limit imposed on either length or diameter. The bivariate length and diameter were recorded individually for each object measured. Fibers were defined as any object that had an aspect ratio of at least 3:1. The diameter was determined at the greatest width of the object. All other objects were considered as nonfibrous particles. The stopping rules for counting of each sample were defined as follows: For nonfibrous particles, the recording of particles was stopped when a total of 30 particles were recorded. For fibers, the recording was stopped when 500 fibers with length $\geq$5 μm, diameter $\leq$3 μm (WHO, 1985), or when a total of 1000 fibers and nonfibrous particles was recorded. If this number of fibers was not reached after evaluation of 0.15 mm^2 of filter surface, additional fields of view were counted until either 500 WHO fibers was reached or a total of 5 mm^2 of filter surface was evaluated, even if a total of 500 countable WHO fibers was not reached. The evaluation of short fibers (length $<$5 μm) was stopped when 100 short fibers was reached.

Confocal Microscopy

On a further subgroup of animals, the lungs (sectioned below the larynx) were collected, and the attached mediastinal tissue was resectioned from the lung lobes and discarded. The whole lungs including tracheobronchial tree were weighed. The lungs were fixed in Karnowsky solution and sent to Rogers Imaging Corporation (Needham, MA) for analysis by confocal microscopy.

Confocal microscopy was performed using a Sarastro 2000 (Molecular Dynamics, Inc.) laser scanning microscope fitted with a 25-mW argon-ion laser and an upright microscope (Optiphot-2; Ni0n, Inc.) modified for enhanced reflected light imaging. Fluorescently labeled cellular constituents (Rogers et al., 1999). and reflective/ refractive fibers (and particles) were imaged simultaneously with this arrangement. Each "exposure" produced two digital images.

An image recorded in either mode was a two-dimensional (x, y), 512 $\times$ 512 array of pixels, each with an intensity value from 0 to 254 gray scale units (a value of 255 indicated saturation of the intensity scale). Optical (x, y) sections, individually and in depth series, were recorded at various positions along the z axis by adjusting the stage height using stepper motors under computer control. Images and image series were analyzed and prepared for presentation by employing specialized computer software.

Images were recorded through a 40$\times$ objective. The dimensions of voxels in the recorded volume were (x, y, and z dimensions, respectively) 0.126 μm, 0.126 μm, and 0.3 μm. The dimensions of each recorded volume were: 64.5 μm $\times$ 64.5 μm $\times$ 7.5 μm, giving 31145 μm^3 of lung parenchyma recorded per section series.

Morphometric Methods

The numbers of fibers within various anatomical compartments were determined by confocal microscopy employing serial optical section techniques. The sampling strategies were designed to permit the determination of the number and location of fibers retained within the parenchyma and the conducting airways.

Sampling Strategy for Parenchyma. As parenchyma provides about 90% of the lung's volume and varies little if at all from one region of the lung to another, it is readily possible to acquire random fields-of-view of parenchyma from which quantitative data may be obtained. Our procedure was to place the microscope objective at random over the lung specimen exposed at the surface of the epoxy embedment, collect a depth series of images, return to the initial starting depth, move two field widths in the positive x direction, and repeat the process. Twenty depth series were obtained in this way from each piece of lung examined (four per animal). If the perimeter of the lung section was encountered, the objective was moved two field widths in the positive y direction, and the stepping was continued in the negative x direction. At each location, if the profile of a conducting airway was in the volume to be recorded by the depth series, the field-of-view was skipped, and another step was made, until a volume was found that did not contain an airway. Each volume was recorded by obtaining 25 optical sections separated by 0.3 μm along the z axis.

Fibers in each volume were detected by scanning up and down through the depth series of images while looking for the characteristic bright points or lines that indicated a reflective or refractile fiber or particle. The person counting fibers did not know which experimental group the images were drawn from; that is, the counting was done under "single blind" conditions. These

counts provided data with units of number of fibers per volume of parenchyma in cubic micrometers. Knowing the volume represented by each depth series and the volume of parenchyma (including airspaces) in the animal's entire lungs, as fixed, the fiber load in the lung's parenchyma could be calculated. The anatomic compartment in which the fiber occurred was recorded. Fibers in parenchyma were classified as occurring in alveoli, alveolar ducts, or respiratory bronchioles, in contact with the surface of tissue, in alveolar ducts or alveoli, but not in contact with tissue in the recorded volume, wholly or partly inside alveolar macrophages.

Sampling Strategy for Airways. Airways occupy only 10% of total inflated lung volume and exist as a treelike structure that is relatively coarse compared to parenchymal structures. Therefore, a field-of-view positioned at random on a lung sample has a rather low probability of containing any airway wall profile. Instead, it was efficient and valid to proceed along a randomly positioned line on the lung sample's surface and record volumes whenever the line encountered an airway whose local axis was nearly enough parallel to the sample surface's normal that the tissue layers in the airway wall were readily discerned. Five depth series (dimensions identical to parenchymal depth series) were recorded from each of 4 lung pieces per animal, and these stacks held, on average, 75.2 μm of airway wall profile each.

Inflammatory Cells. Inflammatory cells expected to occur in the alveolar airspaces would be, for example, neutrophils. Efficient random sampling strategy designed to reveal the distribution of fiber load also revealed the nature of inflammatory cells in context with fibers and permitted unbiased observations of this pulmonary compartment.

RESULTS

Validation of Lung Digestion Procedure

The confocal microscopy procedure is relatively noninvasive, as a cube of the lung is analyzed in three dimensions and the method requires no physical thin sectioning of the lung tissue. To assure that the lung digestion and transmission electron microscopy (TEM) procedures used in this study did not affect recovery of the chrysotile fibers present in the lung, the results obtained with the lung digestion/TEM procedure were compared with those obtained using confocal microscopy. The results of this analysis confirmed that there is a very good correlation between the total fiber number in the lung as measured by the lung digestion procedure/TEM and the confocal methodology. In the medium dose the correlation coefficient between the two methods was $r^2 = .92$ and in the high dose the $r^2 = .99$, indicating that the digestion/TEM procedure does not effect the number of fibers recovered from the lungs.

Concentration and Fiber Size Distribution in the Exposure Aerosol

The inhalation exposure was performed as planned for the 90-day exposure period. The mean gravimetric aerosol concentration and the corresponding mean number of fibres per cubic centimeter in the exposure atmosphere are presented in Table 3. The bivariate fiber dimensions were determined twice during the first week of exposure and once a week thereafter. The gravimetric concentration was determined daily. The mean fiber aerosol dimensions are shown in Table 4.

TABLE 3
Mean gravimetric aerosol concentration and the corresponding mean number of fibers per cubic centimeter in the exposure atmosphere

	Mean gravimetric concentration (mg/m^3)		Fiber number (fibers/cm^3)		
Group	Target	Achieved $\pm$ SD	Total	WHO	L > 20 μm
Medium	1.3	1.32 ± 0.06	3413	536	76
High	3.3	3.56 ± 0.37	8941	1429	207
Ratio high/medium	2.5	2.7	2.6	2.7	2.7

Note. Total = all objects with a 3:1 aspect ratio (minimum) without any limits for length and diameter. WHO = fibers $\geq$5 μm in length and $\leq$3 μm diameter. SD, = standard deviation of weekly means (wk 1–13).

The fiber exposure concentrations were initially chosen based on a prestudy calibration trial to be 50 and 150 fibers/cm^3,

TABLE 4
Mean fiber dimensions of the medium and high dose chrysotile aerosol exposure

	CA300 medium dose	CA300 high dose
Diameter		
Range (μm)	0.03–1.1	0.03–2.7
Geometric mean (μm)	0.14	0.15
Geometric standard deviation	1.98	1.97
Arithmetic mean (μm)	0.16	0.17
SD	0.10	0.11
Geometric mean (μm)	0.14	0.15
SD	1.98	1.97
Median (μm)	0.15	0.15
Length		
Range (μm)	0.6–110	0.7–130
Geometric mean (μm)	2.87	2.89
Geometric standard deviation	4.21	4.27
Arithmetic mean (μm)	4.00	4.07
SD	16.53	17.05
Geometric mean (μm)	2.87	2.89
SD	4.21	4.27
Median (μm)	2.5	2.5

which correspond in the EC subchronic fiber inhalation protocol (Bernstein & Riego-Sintes, 1999) to the medium and high dose levels recommended for exposure. However, due to variation in the distribution of the stock fiber, the mean high dose fiber exposure concentration was 207 f/cm^3 $L > 20$ μm and the medium dose was 76 f/cm^3 $L > 20$ μm.

Fiber Lung Burden and Clearance

The fiber lung burdens of subgroups of animals analyzed following the end of the 90-day exposure period and after 50 days and 92 days of exposure-free recovery are summarized in Tables 5 and 6 for the medium and high dose, respectively.

TABLE 5
Fiber lung burden—medium dose

Sacrifice time point	After 90-day exposure	After 50-day recovery	After 92-day recovery
Fiber number (in millions of fibers)			
Total fibers/lung	147.1	25.6	21.5
Total fibers/g ww lung	91.9	15.2	12.7
WHO fibers/lung	19.7	6.1	5.4
WHO fibers/g ww lung	12.3	3.6	3.2
Fibers $L > 20$ μm/lung	0.6	0.10	0.10
Fibers $L > 20$ μm/g ww lung	0.38	0.06	0.06
Fibre diameter			
Range (μm)	0.03–0.70	0.03–0.80	0.03–1.8
Arithmetic mean (μm)	0.10	0.11	0.11
SD	0.06	0.07	0.08
Geometric mean (μm)	0.08	0.09	0.09
SD	7.72	7.72	7.72
Median (μm)	0.08	0.08	0.08
Fiber length			
Range (μm)	0.7–90	0.8–48	1.0–48
Arithmetic Mean (μm)	3.50	4.30	4.20
SD	2.80	3.20	3.00
Geometric mean (μm)	2.90	3.50	3.50
SD	3.50	3.50	3.50
Median (μm)	2.8	3.3	3.3
Fibre volume and surface			
Mean volume (μm^3)	0.06	0.09	0.09
SD	0.014	0.015	0.016
Total volume (mm^3)	0.008	0.002	0.002
SD	0.001	0.001	0.0004
Mean surface area (μm^2)	1.29	1.73	1.79
SD	0.248	0.307	0.154
Total surface area (cm^2)	1.81	0.46	0.38
SD	0.247	0.254	0.086
Aspect ratio	46.4	44.6	45.4
Total length (m)	509.2	109.1	89.5

Note. ww, Wet weight.

TABLE 6
Fiber lung burden—high dose

Sacrifice time point	After 90-day exposure	After 50-day recovery	After 92-day recovery
Fibre number (in millions of fibers)			
Total fibers/lung	273.4	50.4	42.8
Total fibers/g ww lung	146.2	26.4	23.4
WHO fibers/lung	45.8	12.3	10.7
WHO fiber/g ww lung	24.5	6.4	5.9
Fibers $L > 20$ μm/lung	1.10	0.20	0.20
Fibers L > 20 μm/g ww lung	0.59	0.10	0.11
Fiber diameter			
Range (μm)	0.03–2.8	0.03–0.73	0.03–1.2
Arithmetic Mean (μm)	0.13	0.15	0.13
SD	0.09	0.09	0.08
Geometric mean (μm)	0.11	0.12	0.11
SD	7.72	7.72	7.72
Median (μm)	0.12	0.13	0.12
Fiber length			
Range (μm)	0.6–50	0.7–45	0.8–50
Arithmetic mean (μm)	3.50	4.30	4.20
SD	2.90	3.10	3.00
Geometric mean (μm)	2.80	3.60	3.50
SD	3.50	3.50	3.50
Median (μm)	2.6	3.4	3.3
Fiber volume and surface			
Mean volume (μm^3)	0.11	0.13	0.11
SD	0.023	0.019	0.012
Total volume (mm^3)	0.028	0.007	0.005
SD	0.011	0.001	0.001
Mean surface area (μm^2)	1.76	2.30	1.98
SD	0.442	0.190	0.179
Total surface area (cm^2)	4.76	1.15	0.86
SD	2.286	0.159	0.243
Aspect ratio	33.1	36.6	40.4
Total length (m)	949.3	214.9	178.0

The mean lengths in both the medium- and high-dose groups increase from 3.5 μm to 4.2–4.3 μm following cessation of exposure. However, as illustrated in Figure 1 for the medium dose, this is largely a result of the large number of shorter fibers counted at day 0 following cessation of exposure. Similar results were obtained for the high dose length distribution.

While the biopersistence results would suggest a rapid clearance of the long fibers, from Table 6, some do remain through 92 days postexposure. This represents ~0.4% of the total number of fibers. It is possible that with the high exposures in this study, the macrophages can't assist in the breakup of the longer fibers. Therefore it is possible under these conditions to have long fibers remaining, most likely in granulomas. When the lung is digested, these are released.

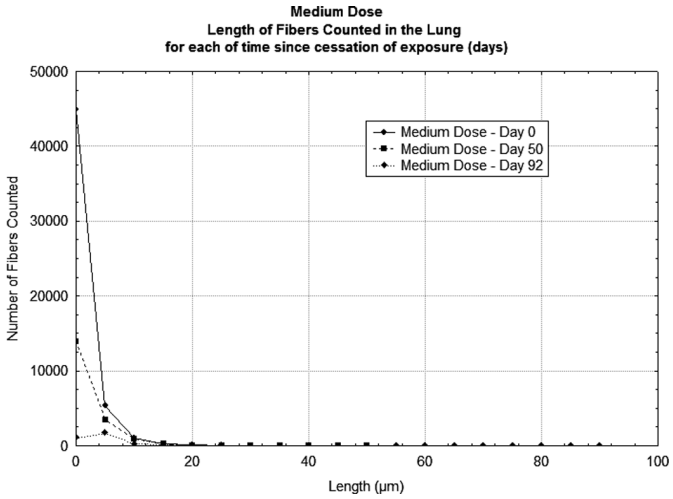

FIG. 1. The number of fibers counted on the filter are shown as a function of fiber length for the medium dose exposure group at each sacrifice time point.

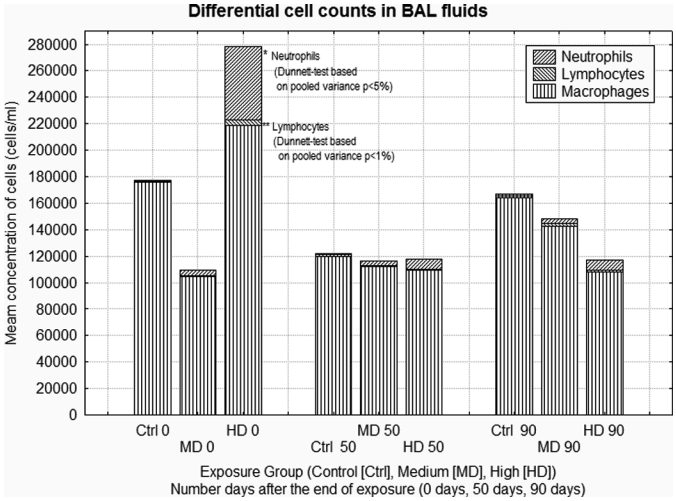

FIG. 2. Differential cell counts determined following bronchoalveolar lavages that were performed on subgroups of five rats for each dose group at each sacrifice time point following cessation of exposure. The mean values that were statistically significant different from the controls are indicated by the asterisks.

IN-LIFE OBSERVATIONS

Body Weights

There were no statistically significant differences in mean body weights or mean body weight gain throughout the exposure and recovery period.

Lung Weights

A dose-dependent increase in lung weights was observed at sacrifice following the 90-day exposure period and after 50 days of recovery. By 90 days of recovery, the difference between groups was no longer statistically significant (Table 7).

Bronchoalveolar Lavage

Bronchoalveolar lavages were performed on subgroups of five rats for each dose group at each sacrifice time point following cessation of exposure. The results from the differential cell counts are shown in Figure 2. The mean values for recovered broncho-alveolar lavage fluid volumes were similar in all groups and there was no adverse effect on cell viability. With the exception of a reduction in the high dose after 92 days of recovery, there were no statistically significant differences in the numbers of macrophages. For neutrophils, there was no statistically significant difference between the medium dose and control at any time point. In the high dose, immediately after cessation of exposure there was a statistically significant increase in neutrophils which was reduced after 50 and 92 days.

Table 8 shows the lactic dehydrogenase (LDH), β-glucuronidase (β-GRS), and total protein results. There were no statistically significant differences in β-glucuronidase with the controls. Again the most notable differences occurred immediately following the cessation of exposure in the high dose LDH (2.8 times control) and total protein. At 50 days there were no statistically significant differences. At 92 days postexposure there were again statistically significant differences for LDH (1.7 times in medium dose and 1.6 times in high dose) and total protein.

TABLE 7
Lung weights(g) (group means/standard deviation)

Time	Control	Medium dose	High dose
After 90 days	1.41	1.60[a]	1.87[b]
treatment	0.07	0.17	0.13
After 50 days	1.46	1.68[a]	1.91[b]
recovery	0.09	0.17	0.25
After 92 days	1.68	1.70	1.83
recovery	0.11	0.12	0.16

[a]Dunnett test based on pooled variance significant at 5% level.
[b]Dunnett test based on pooled variance significant at 1% level.

Cell Proliferation Analysis

The results of the BrdU proliferation analysis are summarized in Table 9. Shown are the cell proliferation results from subgroups of 3 rats from the air control and high dose treatment groups of the 92-day recovery time point. This analysis was performed to provide an indication of the trend between the control and high dose at 92 days after cessation of exposure.

The cell proliferation analysis on rat lungs at the 92-day recovery time point indicates that there is no difference in cellular

TABLE 8
Clinical biochemistry—the lactic dehydrogenase (LDH), β-Glucuronidase, and total protein results [mean (standard deviation) $n = 5$]

	LDH U/L	β- GRS U/ml	PROTEIN T. mg/L
After 3 months of treatment			
Control	59	3.78	37
	(10)	(0.93)	(13)
Medium dose	89	4.38	77
	(15)	(0.45)	(15)
High dose	166[b]	8.40	182[b]
	(42)	(5.82)	(73)
After 50 days of recovery			
Control	96	6.12	91
	(49)	(2.04)	(88)
Medium dose	83	6.49	88
	(21)	(1.73)	(21)
High dose	114	7.89	107
	(39)	(2.91)	(20)
After 92 days of recovery			
Control	66	4.14	41
	(20)	(1.52)	(13)
Medium dose	116[a]	5.43	101[b]
	(22)	(1.51)	(23)
High dose	106[a]	5.97	104[b]
	(32)	(2.44)	(24)

[a]Significantly different from controls (Dunnett test, pooled variance), $p < .05$.
[b]Significantly different from controls (Dunnett test, pooled variance), $p < .01$.

TABLE 9
Proliferation index of lung tissue airway cells after 92 days of recovery

		Exposure group		
Finding	Parameter	Control	Medium dose	High dose
Terminal bronchiole region	Mean	8.0		8.31
	SD	2.19		2.87
	n	3		3
Lung parenchyma	Mean	1.43		1.58
	SD	1.03		0.98
	n	3		3
Pleura (cells/cm)	Mean	22.2		21.3
	SD	8.65		7.24
	n	3		3

Note. Statistics: ANOVA + Dunnett's tests. (two-Sided). No significant differences were observed. *n*: Number of animals. Medium dose, not measured.

TABLE 10
Histopathology findings in the lung: mean severity of findings/group/sacrifice time point

		Exposure group		
Finding	Sacrifice	Control	Medium dose	High dose
Alveolar macrophages	0	0	1.2	1.4
	50	0.2	0.2	0.6
	92	0	0	0.4
Microgranulomas—at the	0	0	1.6	2.0
bronchiolar–alveolar	50	0	0.6	1.8
junction	92	0	1.4	2.0
Alveolar bronchiolization	0	0	0.6	1.2
	50	0	0	0.4
	92	0	0.4	1.2
Fibrosis—at the	0	0	1.0	2.0
bronchiolar–alveolar	50	0	0.8	2.0
junction: 0 none;	92	0	1.2	2.0
1 minimal; 2 slight; 3 moderate; 4 marked; 5 massive				
Wagner score: 1 normal;	0	1.0	2.6	4.0
2–3 cellular changes;	50	1.2	1.8	4.0
4–8 increasing	92	1.0	2.6	4.0
degree fibrosis				
Mean percentage of the	0	0	0.10	1.39
lung with fibrosis	50	0	0.03	1.32
measured per sacrifice	92	0	0.19	1.26

proliferation between the high dose and control groups in the three pulmonary compartments examined: terminal bronchioles, parenchyma, and pleura.

Histopathology Findings in the Lung

A detailed summary of the histopathological findings is shown in Table 10 for the three sacrifice dates. The severity of histologic changes was scored by EPS using a grading system from 1 to 5 with 1 = minimal, 2 = slight, 3 = moderate, 4 = marked, and 5 = massive. A score of zero indicates that this finding was not observed. In addition, the lungs were evaluated using the grading system described by McConnell and Davis (2002), which is a refinement of the original Wagner grading system. Grades 1–3 represent cellular changes, while grades 4–8 represent different degrees of fibrosis starting with minimal collagen deposition at the level of the terminal bronchiole and alveolus (grade 4).

As shown in Table 10, the medium dose chrysotile exposure resulted in a cellular response either immediately after the end of exposure or through the 92-day recovery period (reflected McConnell–Davis [Wagner] grade 3 and EPS grade 1 [very slight]). In the high dose group, a slight degree of

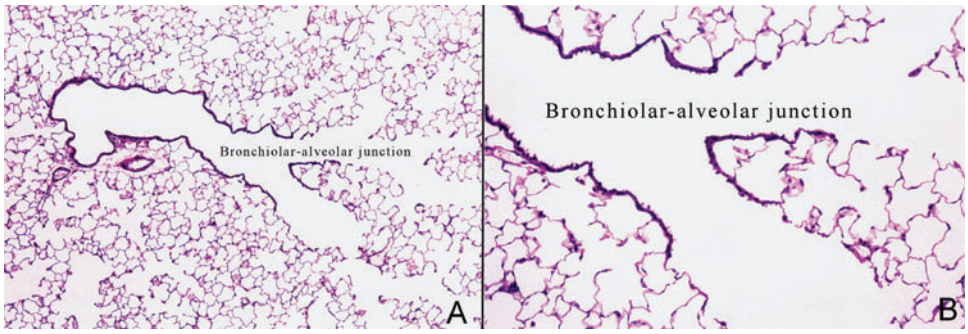

FIG. 3. Control lung: Photomicrographs showing histopathology of the control lungs after cessation of the 90-day exposure. Trichrome stain for collagen specific analysis. (A) 63× (B) 160×.

interstitial fibrosis was observed corresponding to McConnell–Davis (Wagner) grade 4 and to EPS grade 2. In addition, the mean percentage of fibrosis in the lung was evaluated at each sacrifice time point as per McConnell and Davis (2002). The minimal response in the medium dose group was observed in less than 0.2% of the lung. Even in the high dose group, the slight response observed occurred in less than 1.4% of the lung.

Histopathological Results After 90 Days of Exposure

In the control group, Wagner grade 1 was diagnosed in all rats. Photomicrographs of the control lung after cessation of the 90-day exposure are shown in Figure 3.

In the medium dose group, Wagner grade 2 was diagnosed in 2 rats, and Wagner grade 3 was noted in 3 rats. These findings were characterized by alveolar macrophages/microgranulomas at the bronchiolar–alveolar junction. In the rats with Wagner grade 3, alveolar bronchiolization was also noted. In 4 rats, minimal focal fibrosis was noted in the microgranulomas. Since the severity and distribution of this fibrosis was restricted to one or two foci in the microgranulomas, the lesion was scored as Wagner grade 3. The response of the medium dose group after cessation of the 90-day exposure is illustrated in the photomicrographs shown in Figure 4.

In the high dose group, Wagner grade 4 was diagnosed in all rats. This finding was characterized by alveolar macrophages/microgranulomas and alveolar bronchiolization in 4 rats, and slight fibrosis at the bronchiolar-alveolar junction in all rats. The response of the high dose group after cessation of the 90-day exposure is illustrated in the photomicrographs shown in Figure 5.

Histopathological Results After 90 Days of Exposure and 45 Days of Recovery

In the control group, Wagner grade 1 was diagnosed in 4 rats, and grade 2 was diagnosed in 1 rat, while the Wagner grade 2 was characterized by minimal macrophage aggregation.

In the medium dose group, Wagner grade 1 was diagnosed in 1 rat, and Wagner grade 2 was noted in 4 rats. These findings were characterized by alveolar macrophages/microgranulomas at the bronchiolar–alveolar junction. In 3 rats, minimal focal

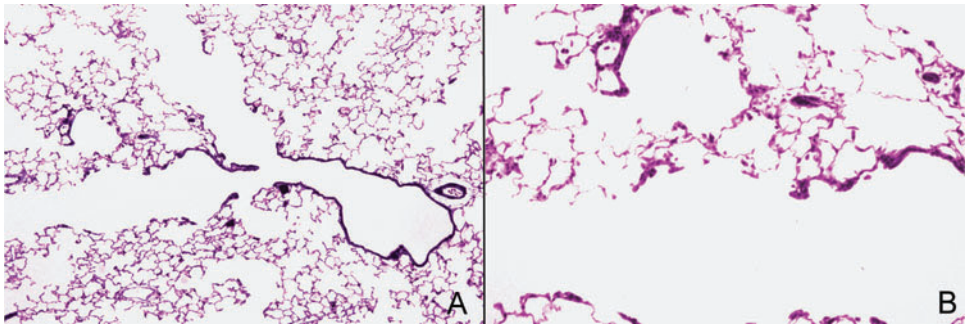

FIG. 4. Medium dose lung: Photomicrographs showing of histopathology of the medium dose lungs after cessation of the 90-day exposure. Trichrome stain for collagen-specific analysis. (A) 63 × , (B) 160 × . A few very small microgranulomas with minimal collagen and a few macrophages are seen.

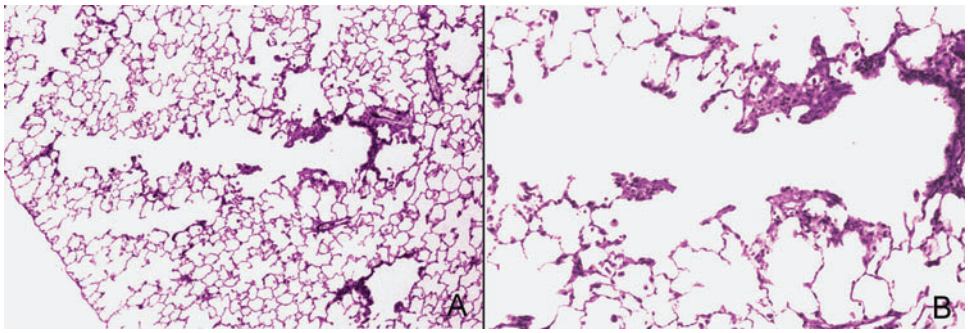

FIG. 5. High dose lung: Photomicrographs showing histopathology of the medium dose lungs after cessation of the 90-day exposure. Trichrome stain for collagen-specific analysis. (A) 63×, (B) 160×. A few small microgranulomas with slight collagen and a few macrophages are seen.

fibrosis was noted in microgranulomas. Since the severity and distribution of this fibrosis was restricted to one or two foci, the fibrosis was considered not to be sufficient for scoring Wagner grade 4.

In the high dose group, Wagner grade 4 was diagnosed in all rats. This finding was characterized by alveolar macrophages/microgranulomas and fibrosis at the bronchiolar–alveolar junction.

Histopathological Results After 90 Days of Exposure and 92 Days of Recovery

In the control group, Wagner grade 1 was diagnosed in all rats.

In the medium dose group, Wagner grade 2 was diagnosed in 3 rats, grade 3 was noted in 1 rat, and grade 4 was noted in 1 rat. These findings were characterized by microgranulomas at the bronchiolar–alveolar junction. In the rat with grade 3, alveolar bronchiolization was diagnosed at the bronchiolar–alveolar junction. In the rat with grade 4, slight fibrosis were noted at the bronchiolar–alveolar junction. In 1 rat, minimal focal fibrosis was noted in microgranulomas. Since the severity and distribution of this fibrosis were restricted to one or two foci, the fibrosis was considered not to be sufficient for scoring Wagner grade 4.

In the high dose group, Wagner grade 4 was diagnosed in all rats. This finding was characterized by alveolar macrophages/microgranulomas, bronchiolization, and slight fibrosis at the bronchiolar–alveolar junction.

Confocal Microscopy

Volume of Lung Tissue Examined—Confocal Microscopical Method Versus Histopathological Examination

In the present investigation, $2.49 \times 10^6 \mu m^3$ of lung was examined by confocal microscopy. The lung tissue sampled for this study was distributed over a region 25 times greater than that typically observed for routine histopathology.

Histological examination is typically limited to structural anomalies of cells or groups of cells with a minimal size of 10 μm. Confocal microscopic analysis as performed in this study was made at a resolution of 0.1 μm, 3 times greater in resolution than that obtainable by traditional histopathological analysis.

Therefore, the tissue volume sampled here was distributed far more uniformly throughout the lung and thus supplied a sample suitable for quantitative analyses. Use of quantitative confocal microscopic analysis produced a detailed examination of fibrils and their association with cells of lung tissue to give robust results in an unbiased fashion.

Appearance of Lung Tissue, Fibers, Alveolar Macrophages, and Neutrophils

Figures 6, 7, 8 and 9 show optical sections through parenchymal regions (Figures 6–8) or airways (Figure 9) from animals from, respectively, the 90-day exposure, 0-day recovery; the 90-day exposure, 50-day recovery; and 90-day exposure, 92-day recovery time groups. Each of these figures shows three columns, with confocal images of lung tissue from the high dose, medium dose, and air control treatment groups, respectively. Figure 8 has two rows showing (upper row) free cells located adjacent to (lower row) parenchymal septal tissue.

The typical appearance of macrophages changed over the recovery time course. At 0 days of recovery in medium and high dosage treatment groups (see Figure 6, A and B), macrophages often appeared large and foamy and were occasionally seen in groups. After 50 days of recovery in medium and high dosage treatment groups (see Figure 7, A and B), macrophages were sometimes grouped, but were rarely enlarged and only were foamy when large, which was seldom observed. Foamy macrophages usually were in airways and were perhaps dead and in the process of being cleared. After 92 days of recovery in the medium and high dose groups (see Figure 8, A, C, and E), macrophages did not occur in groups at all, and although their size was occasionally larger than that of the ones in the air control group, typically all macrophages were of similar size (about 10 μm or so in diameter).

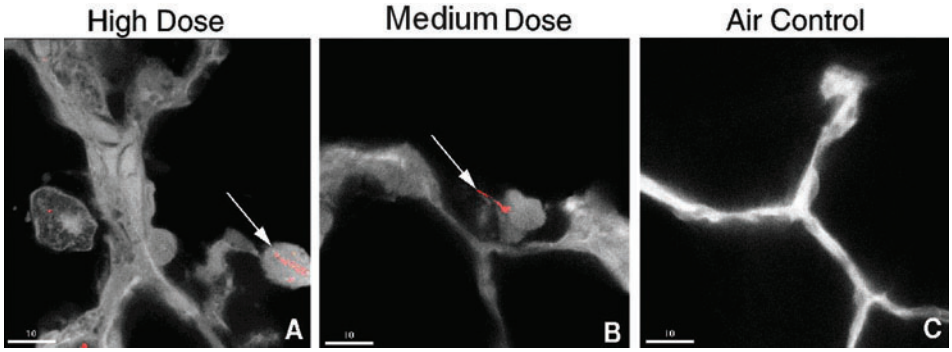

FIG. 6. Confocal micrographs of parenchymal region from representative fields of view recorded from three treatment groups at the 90-day exposure, 0-day recovery time point: high dose (A), medium dose (B), and air control (C). The panels show CA300 fibers (red) fully engulfed (arrow, A) and partially engulfed (arrow, B). Bar represents 10 μm.

In all recovery groups, images recorded (see Figure 9) from the high dose (A), medium dose (B), and air control (C) animals show profiles of airway lumen lined with ciliated cells. Rarely do fibers appear on the lumen surface. When present, CA300 fibers appear as fibril-like material (red) on ciliated cell surface (arrow, Figure 9A) as shown from this panel of images from the 90-day exposure, 92-day recovery group.

Associations Between Macrophages and Particles and/or Fibers

There were occasional groupings of alveolar macrophages, but only in regions where long fibers were present. The number of particles in alveolar macrophages in the medium and high dosage groups dropped 10 to 20-fold over the course of 0 to 92-days of recovery, indicating a constant clearance of very small material from the pulmonary compartment.

Inflammatory Cells

To distinguish between macrophages and neutrophils, such cells were specifically searched for and recorded to view the nucleus in each, crescent-shaped in macrophages and multilobed in neutrophils.

No inflammatory cells were observed in the randomly collected image data used to calculate the compartmentalization of fibers within the lung.

However, to investigate the presence of neutrophils, a deliberate search was conducted of the lung tissue to specifically locate and identify neutrophils. A few neutrophils were observed in alveolar airspaces in the animals in the medium and high dose groups of the 90-day exposure, 92-day recovery time point after exhaustive deliberate searching for this cell type. For example, when searching specifically for neutrophils, approximately 84% of the free cells were alveolar macrophages and 16% of the free cells in alveolar spaces found in the parenchymal region of one high dose lung were neutrophils. Several neutrophils were observed to contain partially engulfed fibers. Deliberate searching in the parenchymal region of the lung from a rat in the medium dose group yielded 97% alveolar macrophages and 3% neutrophils.

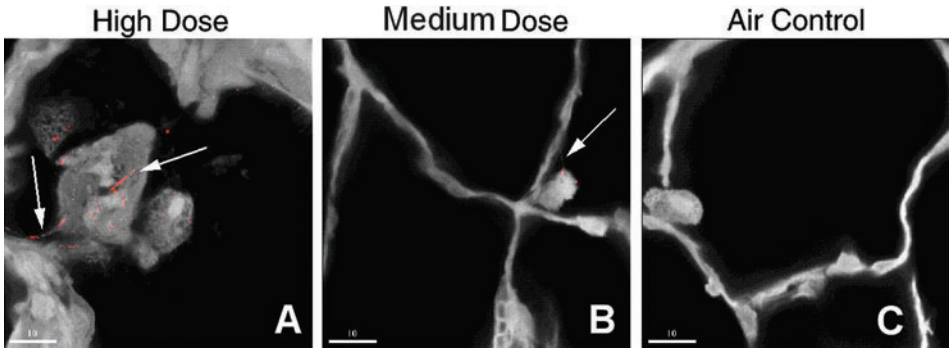

FIG. 7. Confocal micrographs of parenchymal region from representative fields of view recorded from three treatment groups at the 90-day exposure, 50-day recovery time point: high dose (A), medium dose (B), and air control (C). Note CA300 fibers (red) fully engulfed (arrow, A) and partially engulfed (arrow, B). Bar represents 10 μm.

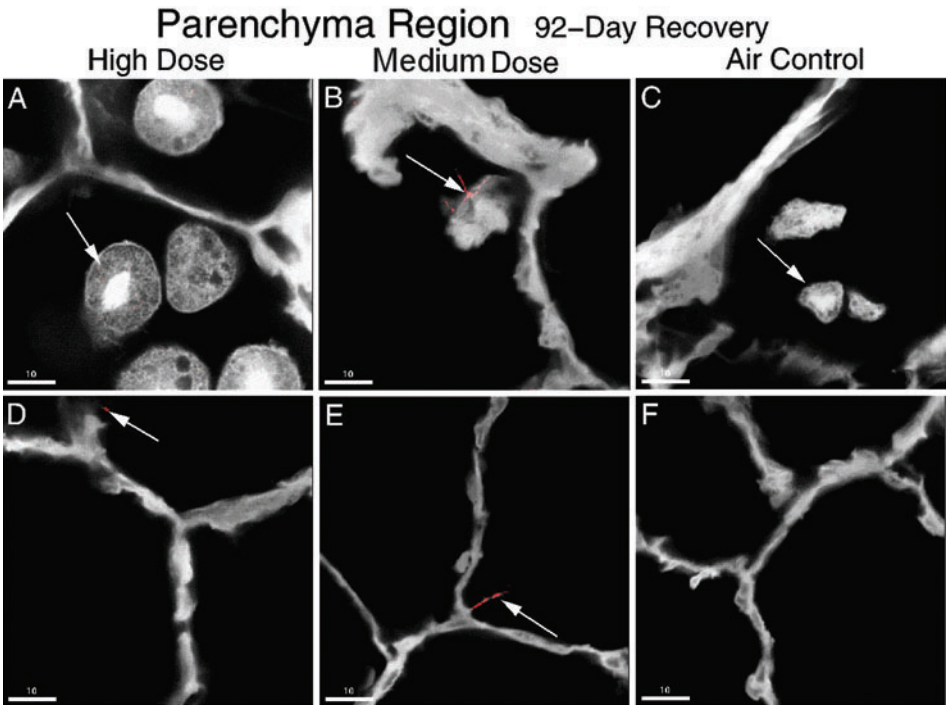

FIG. 8. Confocal micrographs of parenchymal region from representative fields of view recorded from three treatment groups at the 90-day exposure, 92-day recovery time point: high dose (A), medium dose (B), and air control (C). Fine particulate material (red) can se seen inside foamy alveolar macrophages (arrow, A). Occasionally, neutrophils with partially engulfed fibers were observed in alveolar spaces (arrow, B). Alveolar macrophages were occasionally present in the parenchymal region of air control animals (C). Typical parenchymal region fields-of-view (D through F) show alveolar septa and, very rarely, a fiber in contact with the alveolar epithelial surface (E). Bar represents 10 μm.

DISCUSSION

Cellular Response

The differential cell counts obtained following bronchoalveolar lavages indicated that for the medium dose group there was no statistically significant difference in any of the cell counts in comparison to the air control at any of the sacrifice time points.

In the high dose group, immediately after cessation of the 90-day exposure, there was a statistically significant increase in neutrophils and in lymphocytes. By 50 days postexposure, the

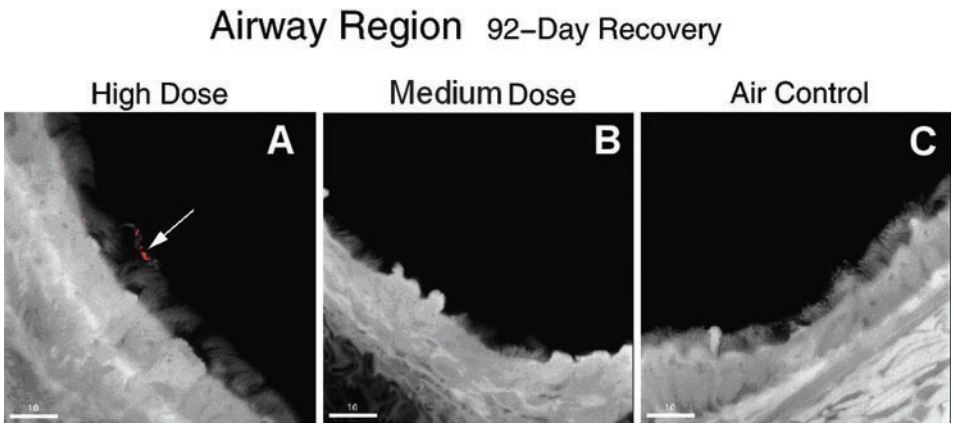

FIG. 9. Confocal micrographs of airway region from representative fields-of-view recorded from three treatment groups at the 90-day exposure, 92-day recovery time point: high dose (A), medium dose (B), and air control (C). These panels show profiles of airway lumen lined with ciliated cells. Fibers rarely appear on the lumenal surface at this time point; finer fibrils (red), when present, appear on ciliated cell surfaces (arrow, A). Bar represents 10 μm.

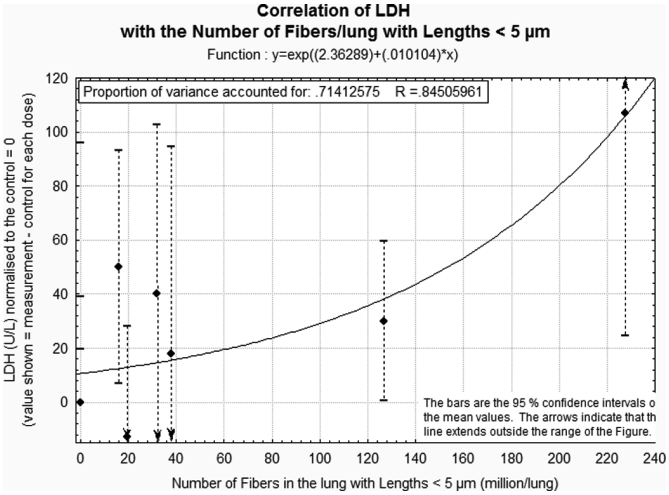

FIG. 10. Correlation of LDH with the number of fibers in the lung with lengths <5 μm. The LDH values were normalized to the control at each sacrifice as indicated. The regression line is shown with statistics. Also shown are error bars indicating the 95% confidence intervals of each mean value.

lymphocyte concentration had returned to normal (not statistically different from control) and was similar at 92 days postexposure. The neutrophils concentration was also reduced at 50 and 92 days but remained at twice the control level.

A similar trend was seen with the clinical biochemistry parameters, LDH and total protein. The mean values for LDH and total protein all were statistically significantly correlated, $p < .01$ (LDH-T. Protein, $r^2 = .96$). Iterative correlation analysis was performed with the number of fibers in the lung using all size fractions, and the best fit was obtained with the number of fibers less than 5 μm remaining in the lung. This relationship is shown in Figure 10 for LDH normalized to the control values at each sacrifice time point ($p = 0.006$; proportion of variance accounted for: .71; $R = .85$). The best fit was obtained with an exponential relationship. These results suggest that the high dose exceeded the ability of the lung to handle the large number of particles and fibers deposited resulting in cell injury as indicated by the LDH increase.

Comparison with other studies of the importance of this increase in LDH is limited due to the number of fibers and the gravimetric mean concentration present in the aerosol exposure (Table 3). Warheit et al. (1992), however, examined the pulmonary cellular effects in rats following aerosol exposures to ultrafine Kevlar aramid fibrils. In this study, the exposure was 6 h/day for only 5 days. The low dose Kevlar fiber exposure was at a mean gravimetric concentration of 2.9 mg/m^3 (high dose in the chrysotile was 3.3 mg/m^3). The mean fiber exposure concentration was 613 WHO fibers/cm^3 (high dose in the chrysotile was 1429 WHO fibers/cm^3). Thus the exposure aerosol was quite comparable. As presented in Figure 6 of Warheit et al., the LDH (as sampled from the BAL) values were 2.8 times control at the end of the 5-day exposure and reached a peak of 5 times control at 72 h. By 1 mo they had returned to the control level; however, at 3 mo postexposure they appeared slightly above control. A similar pattern was seen or total protein (Figure 7 of Warheit et al., 1992). In the current study with chrysotile, the high dose LDH was 2.8 times control at cessation of the 90-day exposure. No statistically significant difference with control was seen at 50 days postexposure and at 92 days postexposure the values in the high dose and medium dose were 1.6 and 1.7 times the control. The LDH values appear to be within what might be considered normal variation for the exposure that occurred.

This is further supported by the observations that:

Medium dose (mean 4413 fibers/cm^3; 536 WHO fibers/cm^3; 76 fibers $L > 20$ μm/cm^3):
- No significant increase in lung neutrophils or lymphocytes (BAL).
- No significant lung fibrosis at any time point.

High Dose (mean 8941 fibers/cm^3; 1429 WHO fibers/cm^3; 207 fibers $L > 20$ μm/cm^3):
- No significant difference in the high dose BrdU levels at 92 days postexposure.
- Increase in lung neutrophils or lymphocytes (BAL) immediately after exposure with subsequent decrease.
- Slight lung fibrosis.

The lung weights (Table 7) immediately after treatment and at 50 days postexposure showed significant increases; however, for the medium dose this represents a 13–15% increase while for the high dose the increase is approximately 30%. By 92 days postexposure, the weights of control and medium dose group were nearly identical and the high dose, while slightly increased, was not statistically different from the control. Such a response is not surprising considering the large number of particles and fibers deposited in the lungs. The increase of the high dose lung weights by greater than 20% would again suggest that the maximum tolerated dose had been exceeded in the high dose.

The cell proliferation as indicated by the BrdU measurements (Table 9) was measured on only 3 out of the 5 rats per group and was measured only at 92 days after cessation of exposure. The 92-days sacrifice was chosen with idea that if there was going to be a progressive response to a "persistent" chrysotile, it would increase over time after cessation of exposure. The results indicate, however, that this was not the case, and the mean values are nearly identical between the high dose at 92 days and the control at the same time.

Biopersistence

Recent publications have clearly shown for synthetic mineral fibers the relationship of biopersistence to both chronic inhalation toxicity and chronic intraperitoneal injection tumour response in the rat (Bernstein et al., 2001a, 2001b). In essence,

if a fiber dissolves rapidly and disappears from the lung, it does not cause a carcinogenic effect. Acceptance of this concept was incorporated, in 1997, into the European Commissions (EC) Directive on man-made mineral fibers (European Commission, 1997). However, neither chrysotile nor amphibole asbestos was included in the analysis performed for the EC and neither one is mentioned in the 1997 directive on synthetic mineral fibers. A recent working group evaluating short-term assays and testing strategies for all types of fibers stated, "Thus the database on the links between in vitro biopersistence, in vivo biopersistence, and pathologic effects is derived for the limited class of silica-based fibers. The extent to which this understanding of biopersistence that we have gained for these fibers is generalizable to other fibers (e.g. organic fibers, crystalline fibers, non oxide fibers is not known and more research is needed before we use the same paradigm for these other fibers types" (ILSI, 2005, p. 508). For these other fibers, the ILSI working group recommended a tiered approach, which included as one of the optional endpoints biopersistence, and recommended subchronic inhalation toxicology study to investigate biological activity.

Chrysotile has been shown to be rapidly removed from the lung following inhalation in experimental animals (Bernstein et al., 2003a, 2003b, 2004, 2005a, 2005b) with clearance of the longer fibers ($L > 20$ μm) ranging from 0.3 to 11.4 days. As mentioned above, studies have shown chrysotile to clear less rapidly (e.g., Coin et al., 1992). In the Coin et al. (1992) study, the NIEHS chrysotile used was derived from a chrysotile product called Plastibest-20, which was a chrysotile used in the plastics industry. The products was ground three times using a "hurricane pulverizer," which is a commercial device designed to grind material under steel. In the Coin et al. studies, an exposure concentration of 10 mg/m^3 was used. Although not stated in the publications, due to the extensive grinding of the Plastibest-20, many more short fibers would be expected. From the LDH and fibrosis results already presented, a more than threefold increase in short fiber number in these studies as compared to the high dose in the present study would certainly be expected to produce an intense inflammatory response. In chronic studies at a concentration of 10 mg/m^3, Bernstein and Hoskins (2005) have shown that this exposure meets the criteria presented by Oberdörster (2002) for lung overload. Besides the studies cited earlier, there have been no other studies examining the clearance of commercial chrysotile products at exposure concentrations even a few orders of magnitude higher than the concentrations found in the workplace.

As chrysotile is a naturally occurring mined fiber, it is not surprising that there are some slight differences in biopersistence, depending on the origin and commercial grade tested. However, across the range of mineral fiber solubilities, chrysotile lies toward the soluble end of the scale and ranges from the least biopersistent fiber to a fiber with biopersistence in the range of glass and stone wools. It is less biopersistent than the ceramic fibers tested or the special-purpose glasses (Hesterberg et al., 1998) and more than 50 times less biopersistent than amphiboles.

The rapid clearance of the long chrysotile fibers from the lung, that is, those fibers that cannot be effectively cleared by macrophages, provides an indication of what may happen when chrysotile is inhaled. While synthetic vitreous fibers (SVF) may dissolve congruently (all component elements dissolving at rates proportional to their mole equivalents in the fibre) or incongruently (leaching with enhanced release of specific elements; Christensen et al., 1994), chrysotile fibers appear to break apart into small particles and smaller fibers. At acidic pH, such as occurs in the macrophage, chrysotile becomes less stable leading to the clearance/disintegration of the long chrysotile fibers. Wypych et al. (2005), have shown in vitro that acid leaching of the chrysotile fibers removes the brucite-like sheets leaving essentially amorphous silica. Disintegration of the fibers provides a basis for understanding the potential toxicity of chrysotile. These results suggest that chrysotile does not act as a fiber in vivo but rather as a particle. The rapid disintegration of the chrysotile fibers would be expected to result in exposure to a large number of amorphous silica particles and shorter fibers.

Chronic Inhalation Studies of Chrysotile

If the primary mode of action of chrysotile at high doses is through an enhanced particle release resulting from the structural collapse of the longer fibers, then the results observed in the chronic inhalation studies of chrysotile should be coherent with those reported for high concentrations of non-fibrous particles.

The exposure concentrations and lung burdens for a series of studies performed with similar protocols on synthetic vitreous fibers and serpentine and amphibole asbestos have recently been evaluated (Bernstein & Hoskins, 2005). The asbestos exposures in these studies were included as positive controls with the exposure concentration based upon 10 mg/m^3 aerosol mass. This resulted for chrysotile in a total fiber aerosol exposure concentration of 102,000 fibers/cm^3 with 10,600 WHO fibers/cm^3 (Hesterberg et al., 1993). The corresponding lung burden was 54,810,000,000 fibers/lung after 24 m of exposure.

The concept of overload of particle-induced pulmonary tumor in the rat has been discussed extensively (Morrow, 1988, 1992; Oberdörster et al., 1992; Oberdörster; 1995a, 1995b, 2002; Bellmann et al., 1992; Hext, 1994). High dose exposure to particulates in the rat has been related to a breakdown of the macrophages' ability to clear the particles that subsequently triggers an inflammatory response that can lead to disease. Bernstein and Hoskins (2005) have evaluated this level of exposure for chrysotile based on these criteria and have shown that lung tumor response in chronic inhalation studies of chrysotile can be accounted for in terms of a high concentration of poorly soluble medium toxicity particles.

Comparative Fiber Number Exposure with Similar Studies

As summarized in Table 3, the mean chrysotile exposure concentration for all fiber lengths was 3413 fibers/cm^3 in the medium dose and 8941 fibers/cm^3 in the high dose exposure group.

TABLE 11
Comparative aerosol exposure characteristics of chrysotile and E-glass, MMVF21, and CMS

Group	Total number of fibers and particles per cm^3	Fibers with length <5 μm per cm^3	Fibers with length = 5–20 μm per cm^3	Fibers with length >20 μm per cm^3	Fibers with length >20 μm; diameter <1 μm, per cm^3	WHO fibers per cm^3	Number particles per cm^3	Gravimetric concentration (mg/m^3)
Chrysotile results from this study								
Chrysotile, medium	3413	2877	460	76	76	536	—	1.3
Chrysotile, high	8941	7512	1222	207	207	1429	—	3.6
E-glass, MMVF21 and CMS results from Bellmann et al. (2003)								
E-glass, low	579	337	181	17	14	198	44	2.4
E-glass, medium	1771	993	572	51	43	623	154	7.0
E-glass, high	5655	3431	1744	142	120	1887	337	17.3
MMVF21, low	131	28	59	17	9	77	26	3.3
MMVF21, medium	372	79	175	58	29	232	61	11.6
MMVF21, high	1176	254	533	174	85	705	217	37.0
CMS, high	3070	287	819	173	105	990	1793	49.5

Bellmann et al. (2003), in a similar 3-mo inhalation study that was based on the same protocol, investigated the biological effects of a special-purpose glass microfiber (E-glass microfiber with exposure concentration for all fiber lengths of 579, 1771, and 5655 fibers/cm^3 in the low, medium, and high dose respectively), a stone wool fiber (MMVF21 with exposure concentration for all fiber lengths of 131, 372, and 1176 fibers/cm^3 in the low, medium, and high dose), and a new high-temperature application fiber (calcium-magnesium silicate fiber, CMS, with exposure concentration for all fiber lengths of 3070 fibers/cm^3 in the high dose) in Wistar rats.

Table 11 presents the comparative aerosol exposure characteristics of the chrysotile from this study and of three fibers used in the Bellmann et al. (2003) study. The high dose chrysotile exposure exceeded, both in terms of the number of fibers $L > 20$ μm and the total particle/fiber exposure per cubic centimeter, the exposure for all three of the fibers studied by Bellmann et al. (E-glass, MMVF21, and CMS).

When comparing the number of fibers with length >20 μm and diameter <1 μm per cubic centimeter, which correspond to fibers that can be inhaled by the rat (rat respirable), the medium dose chrysotile is similar to the high dose CMS. This is of particular importance, as Bellmann et al. (2003) concluded that "The results of the CMS exposure group indicate that effects may be dominated by the presence of nonfibrous particles and that fibrosis may not be a predictor of carcinogenic activity of fiber samples, if the fiber preparation contains a significant fraction of nonfibrous particles (p. 1147)."

The CMS exposure, while similar in fiber number, was at a gravimetric concentration of 49.5 mg/m^3. This is in comparison to the chrysotile medium dose of 1.3 mg/m^3. The reason for this was that the mean CMS dimensions were GMD = 0.88 and GML = 28.9 μm, as compared to GMD = 0.14 and GML = 2.87 μm for chrysotile. The high CMS gravimetric concentration confounds a one-for-one comparison with chrysotile. Studies such as those reported by Gilmour et al. (2004) and Donaldson et al. (2002) suggest that finer material has a greater inflammatory potential.

Comparison of Chrysotile with Synthetic Vitreous Fibers

Even with this possible limitation in interpreting the results from the chrysotile exposure, it is still informative to compare the response of chrysotile to the response of E-glass, MMVF21, and CMS as evaluated with similar protocols. As nearly all the same endpoints were evaluated in both studies, we have in Table 12 reproduced the summary table that was presented by Bellmann et al. (2003) and have added to this table the results for chrysotile from the current study. In addition, to facilitate comparison, we have added in Table 12 the fiber aerosol exposure concentration for the length fraction greater 20 μm and for the total fiber and particulate exposure.

As mentioned earlier, the medium dose chrysotile exposure corresponds in terms of aerosol particle/fiber exposure most closely with the high dose CMS exposure. Even with a higher total particle exposure concentration, the medium dose chrysotile produced less inflammatory response than the similar exposure of CMS. In particular, the medium dose chrysotile exposure resulted in no interstitial fibrosis while the CMS exposure did produce fibrosis.

Even when comparing the high dose chrysotile with more than twice the total particle/fiber exposure to the CMS, while similar levels of fibrosis were noted on the Wagner scale, the chrysotile exposure resulted in a lower PMN response.

TABLE 12
Comparison of chrysotile asbestos with synthetic vitreous fibers: Main findings of different post exposure sacrifice dates

		Chrysotile at sacrifice (wk)			E-glass at sacrifice (wk)			MMVF21 at sacrifice (wk)			CMS at sacrifice (wk)		
Parameter	Dose	0	7	14	1	7	14	1	7	14	1	7	14
Exposure concentration:	Low					579			131				
total fibers and	Medium		3413			1771			372				
particles/cm^3	High		8941			5655			1176			3070	
Fiber exposure conc.:	Low					14			9				
fibers $L > 20$ μm/cm^3	Medium		76			43			29				
with diameter $< 1\mu$m	High		207			120			85			105	
Increase in lung weight	Low												
	Medium		+	+	+++	+++	+	+					
	High		++	++	+++	+++	++	++	++	+			
Biochemical parameters	Low												
in BAL (LDH,	Medium				++	++	+						
β-glucuronidase, protein)	High	+	+	+	+++	+++	++	+++	+	+			+
PMN increase in BAL	Low				+								
	Medium				+++	+++	+	++	+				
	High	+++	+	+	+++	+++	+++	+++	+++	+++		+++	+++
Proliferation of terminal	Low												
bronchiolar epithelium	Medium	N.M.	N.M.	N.M.	+								
	High	N.M.	N.M.		++			++					
Proliferation of alveolar	Low												
parenchymal cells	Medium	N.M.	N.M.	N.M.	++		+						
	High	N.M.	N.M.				++	+					
Proliferation of pleural	Low												
cells	Medium	N.M.	N.M.	N.M.	+								
	High	N.M.	N.M.					+					
Wagner score:	Low				3	2.6	3.2	3	1.4	2			
1 normal, 2–3 focal	Medium	2.6	1.8	2.6	3	3	3.6	3	3	3			
cellular change, 4–8	High	4	4	4	3.75	4	3.8	3.6	3.6	3.5	3	3.6	3.8
increasing degree fibrosis													
EPS score, fibrosis at the	Low				1	0.8	1.2	1	0.2	0			
bronchiolar–alveolar	Medium	1	0.8	1.2	1	1	1.6	1	1	1			
Junction: 0 none;	High	2	2	2	1.75	2	1.8	1.6	1.6	1.5	1	1.4	2
1 minimal; 2 slight;													
3 moderate; 4 marked;													
5 massive													

Note: Blank blocks indicate no exposure for this dose level. N.M.- Indicates no BrdU measurement for this dose level. Significant difference compared to controls (Dunnett test twosided) indicated by +, $p < .05$ or EPS score 1 for fibrosis; ++, $p < .01$ or EPS score 2 for fibrosis; +++, $p < .001$ or EPS score 3 for fibrosis. Adapted from Bellmann et al. (2003), Tables 5 and 15 with the inclusion of the chrysotile results from this study.

When high dose chrysotile is compared to E-glass and MMVF21, the total fiber/particle exposure concentration was 1.6 and 7.6 times greater while the fibers exposure $L > 20$ μm was 1.7 and 2.4 times greater for chrysotile.

Comparison with Amphibole Asbestos

Although comparable results are not available for amphibole asbestos, it is interesting to compare the histopathological response of the amphibole tremolite to that of chrysotile. Bernstein et al. (2005a) reported on the pathological response of tremolite following a 5-day inhalation exposure as part of a biopersistence study. Figure 11, which is reproduced from this publication, illustrates the pulmonary response to tremolite at 90 days following the termination of the 5-day exposure. The tremolite aerosol exposure concentrations were less than that used in the medium does in this study. Comparison with Figure 3b shows that the 5-day tremolite exposure produced a notably more severe reaction that the 90-day chrysotile exposure at a higher aerosol concentration.

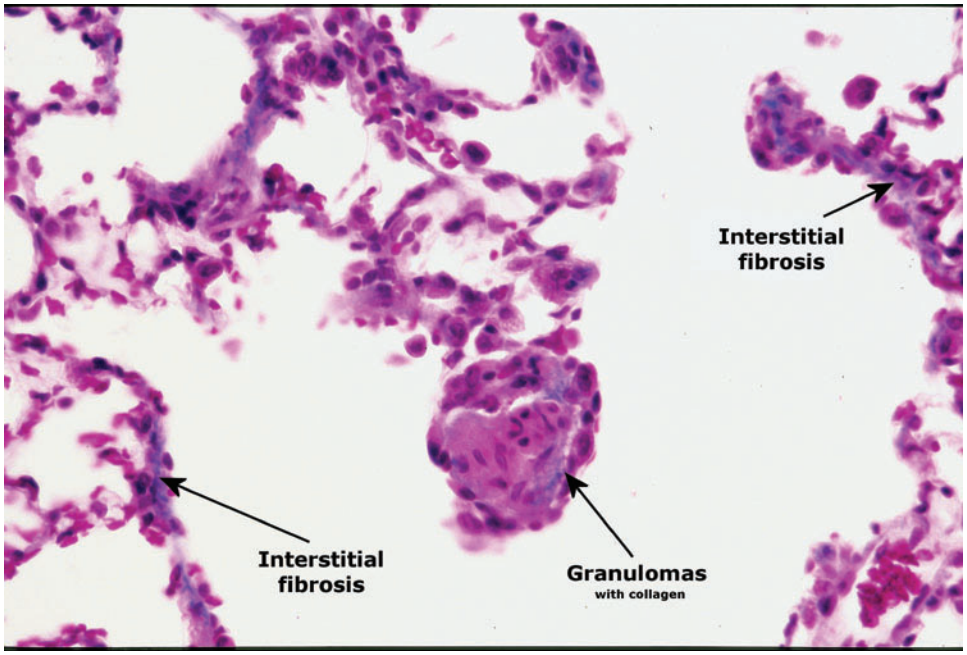

FIG. 11. Photomicrograph of a histopathological section from a tremolite-exposed lung 90 days following cessation of the 5-day exposure. The severity of the fibrosis in the granulomas has increased, and the granuloma can be seen interlaced with collagen. By this time the collagen has progressed into the interstitium and interstitial fibrosis is seen as well. Numerous macrophage aggregates are also observed, as well as multinucleated giant cells. Reproduced from Figure 7, Bernstein et al. (2005a).

Short Fiber Clearance

As detailed in Table 4, and as is characteristic for all fiber exposures, there are many more shorter fibers less than 20 μm in length and even more less than 5 μm in length. Bernstein et al. (2005b) has shown that the clearance of the shorter fibers in biopersistence studies is either similar to or faster than the clearance of insoluble nuisance dusts (Stoeber et al., 1970; Muhle et al., 1987). However, as presented earlier, with all insoluble nuisance dusts, unusually high concentrations can retard clearance and result in the phenomena of lung overload (Bolton et al., 1983; Muhle et al., 1988; Morrow, 1988, 1992; Oberdörster, 1995a, and 1995b, 2002). Even though specific measures of macrophage clearance rates were not undertaken in this study, it is very likely that the chrysotile high dose in the current study has approached or exceeded the level that would produce lung overload. This is supported by the results from the medium dose level, which at 5000 times the U.S.-threshold limit value of 0.1 f (WHO)/cm^3 (ACGIH, 2000) for chrysotile asbestos produces no fibrotic response.

In a recent report issued by the Agency for Toxic Substances and Disease Registry entitled "Expert Panel on Health Effects of Asbestos and Synthetic Vitreous Fibers: The Influence of Fiber Length," the experts stated that "Given findings from epidemiological studies, laboratory animal studies, and in vitro genotoxicity studies, combined with the lung's ability to clear short fibers, the panelists agreed that there is a strong weight of evidence that asbestos and SVFs (synthetic vitreous fibers) shorter than 5 μm are unlikely to cause cancer in humans" (ATSDR, 2003, Executive Summary p. 8; U.S. Environmental Protection Agency, 2003). In addition, Berman and Crump (2003) in their technical support document to the U.S. EPA on asbestos-related risk also found that shorter fibers do not appear to contribute to disease.

CONCLUSIONS

Inhalation toxicology studies with chrysotile asbestos have in the past been performed at exceedingly high doses (usually 10 mg/m^3), using pulverized fibers without full consideration of the impact of the fiber distribution or dimensions. Modeling has suggested that these exposures have exceeded lung overload levels, making quantitative assessment of these studies difficult if not impossible.

This study is the first to assess the cellular and pathological response in the rat lung to a well-characterized aerosol of chrysotile asbestos in a 90-day subchronic inhalation toxicology study. The protocol, based on that established by the European Commission for the evaluation of synthetic vitreous fibers, also was designed to assess the potential for reversibility of any such changes and to permit association of responses with fibre dose in the lung and the influence of fibre length.

Through 90 days of exposure and 92 days of recovery, chrysotile at a mean exposure of 76 fibers $L > 20$ μm/cm^3

(3413 total fibers/cm^3) resulted in no fibrosis (Wagner score 1.8 to 2.6) at any time point. In a similar study on the biosoluble CMS fiber performed at a similar particle/fiber exposure level although at a higher gravimetric level, Wagner grade 4 fibrosis was observed with a moderate increase in PMNs. The authors attributed this to an overload effect due to the large number of particles. The higher chrysotile fiber concentration used in the current study exceeded the particle/fiber concentration used in any other comparable subchronic fiber study in terms of both the number of fibers $L > 20\ \mu$m and the total number of fibers/cm^3.

As predicted by the recent biopersistence studies on chrysotile, this study clearly shows that at an exposure concentration 5000 times greater than the U.S. threshold limit value of 0.1 f(WHO)/cm^3, chrysotile produces no significant pathological response in a subchronic inhalation toxicology study.

REFERENCES

Agency for Toxic Substances and Disease Registry. 2003. *Report on the Expert Panel on Health Effects of Asbestos and Synthetic Vitreous Fibers: The influence of fiber length*. Atlanta, GA: Prepared for Agency for Toxic Substances and Disease Registry, Division of Health Assessment and Consultation.

American Conference of Governmental Industrial Hygienists. 2000. *2000 TLVs and BEIs. Threshold limit values for chemical substances and physical agents and biological exposure indices*. American Conference of Governmental Industrial Hygienists. Cincinnati, OH: ACGIH.

Bellmann, B., Muhle, H. Creutzenberg, O., and Mermelstein, R. 1992. Irreversible pulmonary changes induced in rat lung by dust overload. *Environ. Health. Perspect*. 97:189–191.

Bellmann, B., Muhle, H. Creutzenberg, O., Ernst, H., Muller, M., Bernstein, D. M., and Riego-Sintes, J. M. 2003. Calibration study on subchronic inhalation toxicity of man-made vitreous fibers in rats. *Inhal. Toxicol*. 15(12):1147–1177.

Berman, D. W., and Crump, K. S. 2003. *Technical support document for a protocol to assess asbestos-related risk*. Washington, DC: Office of Solid Waste and Emergency Response, U.S. Environmental Protection Agency.

Bernstein, D. M. 2005. Understanding Chrysotile Asbestos: A New Perspective Based Upon Current Data. In *Proceedings of the International Occupational Hygiene Association, 6th International Scientific Conference, 19–23 September 2005 (IOHA 2005), Pilanesberg National Park, North West Province, South Africa*. http://www.saioh.org/ioha2005/Proceedings.htm

Bernstein, D. M., and Riego-Sintes, J. M. R. 1999. *Methods for the determination of the hazardous properties for human health of man made mineral fibers (MMMF)*. Vol. EUR 18748 EN, April. 93, http://ecb.ei.jrc.it/DOCUMENTS/Testing-Methods/mmmfweb.pdf: European Commission Joint Research Centre, Institute for Health and Consumer Protection, Unit: Toxicology and Chemical Substances, European Chemicals Bureau.

Bernstein, D. M., Mast, R., Anderson, R., Hesterberg, T. W., Musselman, R., Kamstrup, O., and Hadley, J. 1994. An experimental approach to the evaluation of the biopersistence of respirable synthetic fibers and minerals. *Environ. Health Perspect* 102 (suppl. 5): 15–18.

Bernstein, D. M., Riego-Sintes, J. M., Ersboell, B. K., and Kunert, J. 2001a. Biopersistence of synthetic mineral fibers as a predictor of chronic inhalation toxicity in rats. *Inhal. Toxicol*. 13(10):823–849.

Bernstein, D. M., Riego-Sintes, J. M., Ersboell, B. K., and Kunert, J. 2001b. Biopersistence of synthetic mineral fibers as a predictor of chronic intraperitoneal injection tumor response in rats. *Inhal. Toxicol*. 13(10):851–875.

Bernstein, D. M., Chevalier, J., and Smith, P. 2003. Comparison of Calidria chrysotile asbestos to pure tremolite: Inhalation biopersistence and histopathology following short-term exposure. *Inhal. Toxicol*. 15(14):1387–1419.

Bernstein, D. M., Rogers, R., and Smith, P. 2004. The biopersistence of Brazilian chrysotile asbestos following inhalation. *Inhal. Toxicol*. 16(9):745–761.

Bernstein, D. M., Chevalier, J., and Smith, P. 2005a. Comparison of calidria chrysotile asbestos to pure tremolite: Final results of the inhalation biopersistence and histopathology examination following short-term exposure. *Inhal. Toxicol*. 17(9):427–449.

Bernstein, D. M., Rogers, R., and Smith, P. 2005b. The biopersistence of Canadian chrysotile asbestos following inhalation: Final results through 1 year after cessation of exposure. *Inhal. Toxicol*. 17(1):1–14.

Bolton, R. E., Vincent, J. H., Jones, A. D., Addison, J., and Beckett, S. T. 1983. An overload hypothesis for pulmonary clearance of UICC amosite fibres inhaled by rats. *Br. J. Ind. Med*. 40: 264–272.

Cannon, W. C., Blanton, E. F., and McDonald, K. E. 1983. The flow-past chamber: An improved nose-only exposure system for rodents. *Am. Ind. Hyg. Assoc. J*. 44(12):923–928.

Christensen, V. R., Jensen, S. L., Guldberg, M., and Kamstrup, O. 1994. Effect of chemical composition of man-made vitreous fibers on the rate of dissolution in vitro at different pHs. *Environ. Health Perspect*. 102 (suppl. 5) :83–86.

Coin, P. G., Roggli, V. L., and Brody, A. R. 1992. Deposition, clearance, and translocation of chrysotile asbestos from peripheral and central regions of the rat lung. *Environ. Res*. 58(1):97–116.

Cossette, M., and Delvaux, P. 1979. Technical evaluation of chrysotile asbestos ore bodies. In *short course in mineralogical techniques of asbestos determination*, ed. R. C. Ledoux, Mineralogical Association of Canada. Toronto, Ontario 79–110.

Donaldson, K., Brown, D., Clouter, A., Duffin, R., MacNee, W., Renwick, L., Tran, L., and Stone, V. 2002. The pulmonary toxicology of ultrafine particles. *J. Aerosol Med*. 15(2):213–220.

European Commission. 1997. Commission Directive 97/69/EC of 5.XII.97 (23rd adaptation). O.J. L 343/1997.

Gilmour, P. S., Ziesenis, A., Morrison, E. R., Vickers, M. A., Drost, E. M., Ford, I., Karg, E., Mossa, C., Schroeppel, A., Ferron, G. A., Heyder, J., Greaves, M., MacNee, W., and Donaldson, K. 2004. Pulmonary and systemic effects of short-term inhalation exposure to ultrafine carbon black particles. *Toxicol. Appl. Pharmacol*. 195(1):35–44.

Hesterberg, T. W., Miiller, W. C., McConnell, E. E., Chevalier, J., Hadley, J. G., Bernstein, D. M., Thevenaz, P., and Anderson, R.

1993. Chronic inhalation toxicity of size-separated glass fibers in Fischer 344 rats. *Fundam. Appl. Toxicol.* 20 (4):464–476.

Hesterberg, T. W., Chase, G., Axten, C., Miller, W. C., Musselman, R. P., Kamstrup, O., Hadley, J., Morscheidt, C. D., Bernstein, D. M., and Thevenaz, P. 1998. Biopersistence of synthetic vitreous fibers and amosite asbestos in the rat lung following inhalation. *Toxicol. Appl. Pharmacol.* 151 (2):262–275.

Hext, P. M. 1994. Current perspectives on particulate induced pulmonary tumours. *Hum. Exp. Toxicol.* 13(10):700–715.

Hodgson, A. A. 1979. Chemistry and physics of asbestos. In *Asbestos: properties, applications and hazards*, eds. L. M. Chissick and S. S. Chissick, pp. 67–114, New York: John Wiley & Sons.

ILSI. 2005. Testing of fibrous particles: Short-term assays and strategies. Report of an ILSI Risk Science Institute Working Group, *Inhal. Toxicol.*, 17:497–537.

McConnell, E. E., and Davis, J. M. 2002. Quantification of fibrosis in the lungs of rats using a morphometric method. *Inhal. Toxicol.* 14(3):263–272.

Morrow, P. E. 1988. Possible mechanisms to explain dust overloading of the lung. *Fundam. Appl. Toxicol.* 10:369–384.

Morrow, P. E., 1992. Dust overloading of the lungs: Update and appraisal. *Toxicol. Appl. Pharmacol.* 113: 1–12.

Muhle, H., Bellman, B., and Heinrich U. 1988. Overloading of lung clearance during chronic exposure of experimental animals to particles. *Ann. Occup. Hyg.* 32(suppl. 1): 141–147.

Muhle, H., Pott, F., Bellmann, B., Takenaka, S., and Ziem, U. 1987. Inhalation and injection experiments in rats to test the carcinogenicity of MMMF. *Ann. Occup. Hyg.* 31(4B):755–764.

Muhle, H., Bellman, B., and Heinrich, U. 1988. Overloading of lung clearance during chronic exposure of experimental animals to particles. *Ann. Occup. Hyg.* 32(suppl. 1):141–147.

Oberdörster, G. 1995a. Lung particle overload: Implications for occupational exposures to particles. *Regul. Toxicol. Pharmacol.* 21(1):123–135.

Oberdörster, G. 1995b. The NTP talc inhalation study: A critical appraisal focused on lung particle overload. *Regul. Toxicol. Pharmacol.* 21(2):233-241.

Oberdörster G. 2002. Toxicokinetics and effects of fibrous and nonfibrous particles. *Inhal. Toxicol.*, 14(1): 29–56.

Oberdörster, G., Ferin, J., and Morrow, P. E. 1992. Volumetric loading of alveolar macrophages (AM): A possible basis for diminished AM-mediated particle clearance. *Exp. Lung. Res.* 18 (1):87–104.

Rogers, R. A., Antonini, J. M., Brismar, H., Lai, J., Hesterberg, T. W., Oldmixon, E. H., Thevenaz, P., and Brain, J.D. 1999. In situ microscopic analysis of asbestos and synthetic vitreous fibers retained in hamster lungs following inhalation. *Environ. Health Perspect.* 107(5):367–375.

Stoeber, W., Flachsbart, H., and Hochrainer, D. 1970. Der Aerodynamische Durchmesser von Latexaggregaten und Asbestfassern. *Staub-Reinh. Luft.* 30:277–285.

U.S. Environmental Protection Agency. 2003. *Report on the Peer Consultation Workshop to discuss a proposed protocol to assess asbestos-related risk*. Prepared for U.S. Environmental Protection Agency, Office of Solid Waste and Emergency Response, Washington, DC, EPA contract 68-C-98-148, Work Assignment 2003-05. Prepared by Eastern Research Group, Inc., Lexington, MA. Final Report May 30.

Warheit, D. B., Kellar, K. A., and Hartsky, M. A. 1992. Pulmonary cellular effects in rats following aerosol exposures to ultrafine Kevlar aramid fibrils: Evidence for biodegradability of inhaled fibrils. *Toxicol. Appl. Pharmacol.* 116(2):225–239.

World Health Organization. 1985. *Reference methods for measuring airborne man-made mineral fibres (MMMF), WHO/EURO MMMF Reference Scheme*. Vol. EH-4. Copenhagen: WHO.

Wypych, F., Adad, L. B., Mattoso, N., Marangon, A. A., and Schreiner, W. H. 2005. Synthesis and characterization of disordered layered silica obtained by selective leaching of octahedral sheets from chrysotile and phlogopite structures. *J. Colloid Interface Sci.* 283(1):107–112.